Vol. 21, No. 3(2022) Sim2833
Revista Mexicana de Ingeniería Química

Analysis of the thermal efficiency of flat plate solar air heaters considering environmental conditions using artificial neural networks

Análisis de la eficiencia térmica de calentadores solares de aire de placa plana considerando las condiciones ambientales utilizando redes neuronales artificiales

M. Calderón-Ramírez[1], J.A Gomez-Náfate[2], B. Ríos-Fuentes[2], R. Rico-Martínez[3], J.J Martínez-Nolazco[4], J.E Botello-Álvarez[2]*

[1]*Tecnológico Nacional de México. CRODE de Celaya, Departamento de Diseño de Equipo. Diego Arenas Guzmán 901, Zona de Oro, Celaya, Gto. C.P. 38023. México.*
[2]*Tecnológico Nacional de México. Instituto Tecnológico de Celaya, Programa de Doctorado en Ciencias de la Ingeniería. Av. Tecnológico y A. García Cubas s/n, Celaya, Gto. C.P. 38010. México.*
[3]*Tecnológico Nacional de México. Instituto Tecnológico de Celaya, Departamento de Ingeniería Química. Av. Tecnológico y A. García Cubas s/n, Celaya, Gto. C.P. 38010. México.*
[4]*Tecnológico Nacional de México. Instituto Tecnológico de Celaya, Departamento de Ingeniería Mecatrónica. Av. Tecnológico y A. García Cubas s/n, Celaya, Gto. C.P. 38010. México*

Received: May 26, 2022; Accepted: October 7, 2022

Abstract

The variance analysis and Artificial Neural Networks were employed to characterize the thermal efficiency in an Air Solar Heater (ASH), evaluating the effects of the design variables: the depth, material and thickness of the absorber plate and inlet airflow. Using Artificial Neural Networks, it was possible to correlate and estimate the effects of uncontrolled environmental variables on thermal efficiency. Incident solar radiation is the environmental factor with the greatest relevant effect on the thermal efficiency of ASH; due to the inability of the absorber plate to receive, store and transfer the abundant solar energy to the air. The most relevant variables in the design were the material and the thickness of absorbed plate, nevertheless, these variables have opposite behaviors on thermal efficiency under conditions of high and low solar incidence. Under this proposed methodology, it was possible to evaluate and know the effect of the design variables studied, even with the high effect of the prevailing environmental conditions.

Keywords: Solar collector, thermic efficiency, Artificial Neural Network, design parameters.

Resumen

Se empleó el análisis de varianza y Redes Neuronales Artificiales para caracterizar la eficiencia térmica en un Calentador Solar de Aire (ASH), evaluando los efectos de las variables de diseño: la profundidad, el material y el espesor de la placa absorbente y el flujo de aire de entrada. Usando Redes Neuronales Artificiales, fue posible correlacionar y estimar los efectos de las variables ambientales no controladas sobre la eficiencia térmica. La radiación solar incidente es el factor ambiental con mayor efecto relevante sobre la eficiencia térmica de los ASH; debido a la incapacidad de la placa absorbente para recibir, almacenar y transferir la abundante energía solar al aire. Las variables más relevantes en el diseño fueron el material y el espesor de placa absorbida, sin embargo, estas variables tienen comportamientos opuestos sobre la eficiencia térmica en condiciones de alta y baja incidencia solar. Bajo esta metodología propuesta, fue posible evaluar y conocer el efecto de las variables de diseño estudiadas, aún con el alto efecto de las condiciones ambientales imperantes.

Palabras clave: Colector solar, eficiencia térmica, Redes Neuronales Artificiales, diseño de parámetros.

* *Corresponding author. E-mail*: enrique.botello@itcelaya.edu.mx
https://doi.org/10.24275/rmiq/Sim2833
ISSN:1665-2738, *issn-e*: 2395-8472

1 Introduction

Solar energy is clean and abundant. Therefore, solar energy is currently being sought to replace, combine, or complement other forms of conventional fossil energy. In some countries, the policies promote renewable energies such as solar energy in photothermal and photoelectric modalities (Liao *et al*., 2019).

13% of the world's population still does not have access to electricity; a rough estimation of 3 billion people still depends on wood, charcoal, or animal waste as energy for domestic use (ONU, 2015). Power generation is the main factor contributing to climate change, accounting for around 60% of global greenhouse gas emissions. The decarbonization of the energy system should favor the mitigation of the environmental effects caused by the massive use of fossil fuels (IRENA, 2020).

In the United States of America, industrial food production consumes 8.0% of the total energy produced. The operations with the highest energy consumption are heating and drying, cooling and freezing, transport, and mechanical systems (Compton *et al*., 2018). For example, during the industrial drying of food, between 3.00 and 16.00 MJ is consumed per kg of evaporated water (Sanjuan *et al*., 2014).

Solar irradiation can reach values of up to 1200 W/m^2 and is considered abundant, renewable, available, and accessible energy, but at the same time, it is also considered dispersed and discontinuous. Therefore, various devices have been built, such as Air Solar Heaters (ASH), which heat the air in solar or hybrid dryers (Kumar *et al*., 2016). The basic shape of an ASH is a rectangular prism with a base-height ratio of close to three and a shallow depth. A glass cover overlay the ASH, and at the bottom is placed a black metallic plate. The absorber plate can be smooth or corrugated to improve air-surface contact (Singh Bisht *et al*., 2018). The air flows by free or forced convection between the plate and the glass while it is heated by conduction in contact with the hot plate. The thermal efficiency of a solar collector is the fraction of energy transferred to the air of the incident solar energy. In the literature, values from 25 to 75% are functions of the solar incidence, geometric, operational factors, surface, thermal and geometric characteristics of the absorber plate (Abuşka, 2018; Singh Bisht *et al*., 2018).

The thermal efficiency of ASH depends on environmental conditions such as solar irradiation, ambient temperature, wind speed, and relative humidity, among others (Liao *et al*., 2019). Due to this design problem, various authors have created analysis methods that identify the fundamental behavior of the design variables on the ASH, reducing the effect or noise that environmental variables produce on the system. Artificial Neural Networks (ANN) is an effective mathematical method. It developed formulas based on ANN that allow determining the efficiency of flat plate ASHs, with input variables as the surface temperature in the collector, date, time, solar radiation, azimuth angle, and inclination angle (Sözen *et al*., 2008).

The difficulty in analyzing the performance of an ASH is the unknown effect of environmental conditions on thermal efficiency. Experiments under artificial solar incidence have been developed to evaluate the uncertainty associated with ASH due to environmental conditions. These studies have managed to control irradiance levels, finding that the most contributing variable in uncertainty to efficiency is the irradiance level (Sowmy *et al*., 2017). However, these studies do not present a complete view of ASH under full-time operation conditions.

It has been verified that the use of intelligent mathematical models to simulate the thermal performance of ASH under uncontrolled environmental conditions. For example, the ANN model was used to predict the outlet temperature in the solar collector using measured data of solar irradiation, ambient temperature, inlet temperature, and flow of the working fluid. (Diez *et al*., 2019). Furthermore, the performance of a direct absorption nanofluid-based solar collector has been determined using a multi-layer perceptron ANN (Elsheikh *et al*., 2019). Nine collector prototypes were made to feed their model with experimental tests and investigate the effect of absorber plate depth and length on thermal performance. In this case, it was shown that varying the depth from 5 to 15 mm increases the collector's efficiency by 9%. Thus, ANN is shown to be a feasible technique for predicting the performance of renewable energy systems, specifically in the thermal efficiency of air solar heaters (Delfani *et al*., 2019).

In this work, the influence of geometric characteristics, operating variables, and climatic conditions on the thermal efficiency of an ASH with a smooth absorber plate is analyzed by two different strategies, variance analysis and Artificial Neural Networks. The main challenge was to develop

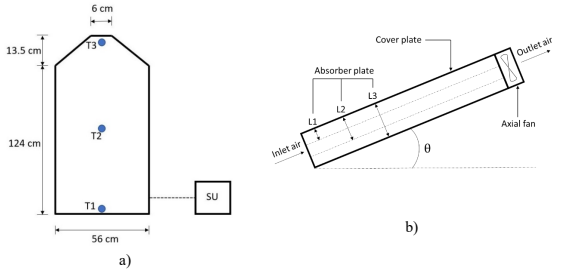

Figure 1. a) The Front view of the solar absorber, b) The lateral view of the solar absorber.

a robust methodology that allows estimating the effects of the design and operating variables on the thermal efficiency of the ASH without the bias of uncontrollable environmental conditions. The strategy consisted of the ASH simulation using an ANN capable of representing and predicting thermal efficiency under different scenarios considering an average global efficiency.

2 Methodology

2.1 Experimental array

A ¾-inch pine wood frame air solar heater was constructed with an aluminum angle rail design that allows the absorber plates to be placed at different depths and interchange and overlap plates of different materials. Smooth metal plates made of galvanized steel, black steel, and 18-gauge aluminum (1.2mm thick) were used as absorber plates. The air inlet is rectangular, 50 cm long, and 5 cm high; the air outlet is a 5 cm diameter circular nozzle. The metal plates and the wooden housing were painted with black acrylic enamel. Figure 1 a) shows a prototype diagram with the main dimensions in the front view and the temperature sensors' position, and Figure 1 b) shows the prototype in the lateral view.

2.2 Data register

Solar radiation was measured with a solarimeter (*Anaheim Scientific, M140*) placed on the surface of the absorber glass plate. Air humidity at the absorber inlet was measured with a hygrometer (*Anaheim Scientific, H300*). The air velocity was measured with a hot wire anemometer (*Twilight LT-AM4216*). The volumetric flow through the absorber was adjusted with the speed of an axial fan (*Manhattan 3-pin*). The temperature was registered with three thermocouples (*Dominion® Type J TCX 100-ECO*) placed at the absorber's inlet, middle, and outlet. The data of the measured variables were stored and processed on a *Raspberry Pi* 4 card. The data sampling and recording were recorded every 15 minutes. The density, viscosity, and thermal conductivity properties of air were estimated by mathematical correlations (Bahrehmand & Ameri, 2015).

2.3 Experimental design

Four factors were taken into consideration at 3 study levels each. Plate depth placed at 5, 10, and 15 cm on aluminum angle rails; absorber plates material, galvanized steel, black steel, and 18-gauge aluminum (1.2 mm thick), where the thermal conductivity of black steel is 63 W/mK, galvanized steel is 76.2 W/mK

Table 1. Controllable factors and levels in the experimental design.

	Factor	Unity	Level	Range
1	Plate depth	[m]	1	0.05
			2	0.1
			3	0.15
2	Absorber plate material	[W/mK]	1	Black steel sheet (63 W/mK)
			2	Galvanized sheet (76.2 W/mK)
			3	Aluminum (210 W/mK)
3	Plate thickness	[mm]	1	1.2
			2	2.4
			3	3.6
4	Volumetric flow in feed	[m^3/s]	1	0.005
			2	0.007
			3	0.009

Table 2. Experimental configuration of the L9 Taguchi-type design.

Experiment number	Setting			
	Plate depth [m]	Plate material [W/mK]	Plate thickness [mm]	Airflow [m^3/s]
1A-1B	0.05	63	1.2	0.005
2A-2B	0.05	76.2	2.4	0.007
3A-3B	0.05	210	3.6	0.009
4A-4B	0.1	63	2.4	0.009
5A-5B	0.1	76.2	3.6	0.005
6A-6B	0.1	210	1.2	0.007
7A-7B	0.15	63	3.6	0.007
8A-8B	0.15	76.2	1.2	0.007
9A-9B	0.15	210	2.4	0.005

and aluminum is 210 W/mK; the thicknesses of the absorbent plates were 1.2, 2.4 and 3.6 mm; volumetric airflow in the feed 0.005, 0.007and 0.009 m^3/s. The absorber was covered with a transparent flat glass plate. Table 1 presents the factors and levels considered studied in the design of experiments.

Due to the long periods in the experimentation time, a fractional Taguchi-type design (L9) of 4 factors was implemented at 3 study levels. The number of experiments was 9 (Table 2), and each experiment was performed in duplicate. The experiments were carried out in October and November 2019, in the courtyard of the National Technological Institute of Mexico in Celaya (20 ° 31'44" N 100 ° 48'54" W), without the presence of buildings or objects that interfere with the solar incidence. The absorber was placed in a south to north orientation with an inclination angle to the horizontal of 30°. The duration of the experiments was considered from 9:00 to 17:00.

The response variable was the daily arithmetic average of thermal efficiency. Thermal efficiency was calculated every 15 minutes, considering the operating and environmental variables recorded during the experiment. Thermal efficiency was evaluated as described in equations 1, 2, and 3.

In equation 1, the thermal efficiency is defined as the relationship between the heat absorbed by the air current that flows through the absorber, "useful heat gained," $\dot{Q}_{useful}$ and the solar energy incident on the plate ($\dot{Q}_{rad}$) (Sharma *et al*., 2018).

$$\eta = \frac{\text{Useful heat gained}}{\text{Incident solar energy}} = \frac{\dot{Q}_{useful}}{\dot{Q}_{rad}} \tag{1}$$

The "useful heat" was calculated from equation 2, where $\dot{m}$ and C_p are the air's mass flow and heat capacity, respectively, $T_{f,o}$ and $T_{f,i}$ are the outlet and inlet temperatures of the air to the absorber.

$$\dot{Q} = \dot{m}C_p\left(T_{f,0} - T_{f,i}\right) \tag{2}$$

The amount of incident heat on the collector ($\dot{Q}_{rad}$) is determined according to equation 3, where A_p the absorber plate area I_T is the solar irradiation area.

$$\dot{Q}_{rad} = A_p I_T \tag{3}$$

2.4 *Artificial Neural Network simulation*

The experimental data of thermal efficiency were correlated utilizing a neural network using MATLAB®. The feedforward type network was used, a propagation network of one hidden layer with 12 neurons, with a sigmoidal transfer function and an output neuron with a linear transfer function. The training method used was a Levenberg-Marquardt (LM) type supervised fit. This iterative technique allows locating the minimum of a multivariate function expressed as the sum of squares of non-linear real-valued functions. LM is considered a steeper descent combination with the Gauss-Newton method. When the current solution is far from correct, the algorithm behaves like a steeper descent method: it is slow, but it guarantees convergence. When the solution is close to the correct solution, it becomes a Gauss-Newton method.

Eight inputs were defined in the Artificial Neural Network. Four controllable represent the design parameters, and the environmental variation acquired four non-controllable. The four controllable inputs were volumetric flow, thermal conductivity, the distance between plates, absorber plate thickness, and the four uncontrollable environmental inputs were ambient temperature, solar radiation, wind speed, and relative humidity.

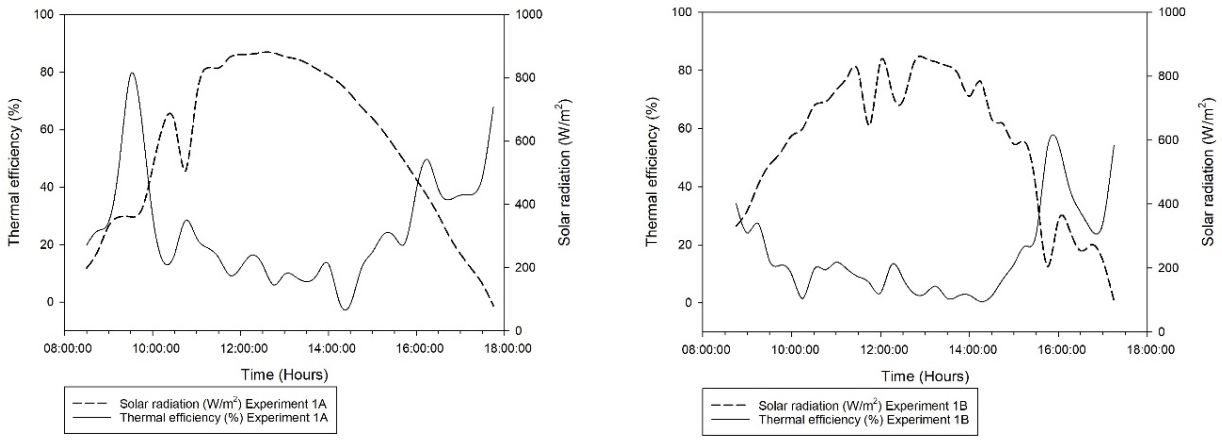

a) b)

Figure 2. Relation of the Thermal efficiency versus the solar radiation, with the configuration of experiment 1 (0.05 m depth, 63 W/mK conductivity, 1.2 m thickness, 0.005067 m^3/s airflows), on two different days.

Thermal efficiency was defined as the output of the system. The gathered data was preprocessed to reduce experimental misleading; the negative efficiencies and the non-usual efficiencies were omitted, with values higher than 150% of efficiency.

The experimental sets (Table 2) were simulated with the neural network considering environmental conditions of the days of maximum (C1) and minimum solar radiation (C2) assessed during the development of the experiments. The principal effects of the factors (Montgomery, 2004): plate depth, plate material, the thickness of the absorber plates, and inlet airspeed were estimated. The average efficiencies were obtained from the simulations of the experimental environmental data with the parameter input in the developed neural network.

Finally, to determine under which conditions those shown in Table 2, the highest average efficiency is obtained regardless of the environmental conditions. Therefore, each run in Table 2 was simulated under all environmental conditions recorded in runs 1A through 9B.

3 Results

3.1 Effect of the environmental variations on the efficiency

The four parameters considered in this study were ambient temperature, solar radiation, wind speed, and relative humidity. The ambient temperature and the solar radiation are factors that influence the effect of the efficiency directly. These two parameters guide the effect of the efficiency and have highly related to each other. The wind speed and the relative humidity are secondary factors with minor effects; these two parameters can alter the efficiency but in combination with the main parameters.

In the statistical analysis of environmental data and thermal efficiency, it was found that solar incidence has the highest correlation coefficient with thermal efficiency -0.4458. In Figure 2 was observed that before noon there is a progressive increase of solar radiation and a consistent decrease in thermal efficiency; besides, in the afternoon, this behavior changes, the solar radiation decreases, and the thermal efficiency increases. This expected result is because the heat transfer between smooth plates and the air stream shows low heat transfer coefficients and has a limited ability to absorb, store and transfer heat energy. Therefore, when solar radiation increases, extra energy is not absorbed. On the other hand, this design has low thermal efficiency because of the low thermal conductivity between the absorber plate and air (Abuşka, 2018). Each experiment was done by duplicate to avoid the experimental misleading due to the environmental variations. In Figure 2, experiment 1A corresponds to the first day in the configuration designed for this experiment. Experiment 1B is made on the tenth day when the environmental conditions are eventually different.

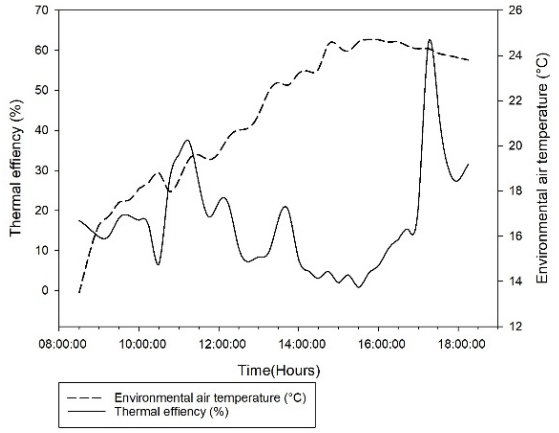

a) Experiment 7A

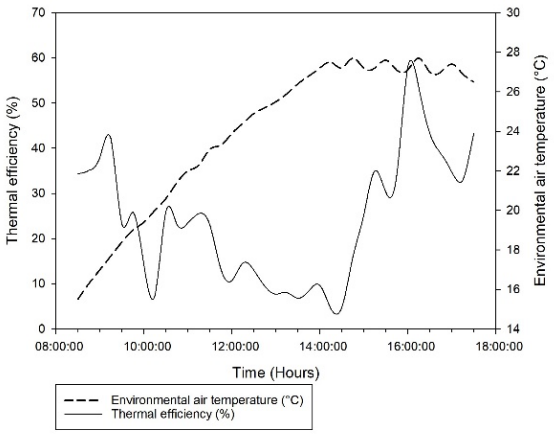

b) Experiment 7B

Figure 3. Effect of the environmental air temperature and the efficiency, with the configuration of experiment 7 (0.15 m depth, 63 W/mK conductivity, 3.6 m thickness, 0.007093921 m^3/s airflows) on two different days.

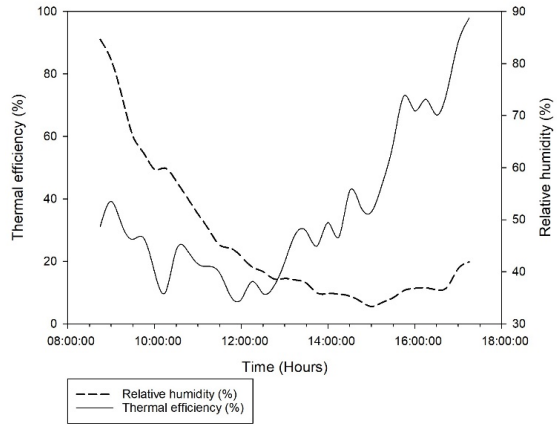

Figure 4. Effect of the Relative humidity and the efficiency, with the configuration of experiment 6 (0.1 m depth, 76.2 W/mK conductivity, 1.2 m thickness, 0.007093921 m^3/s airflows) on two different days.

The temperature variation directly affects the efficiency of this kind of solar absorber. This variation provokes that the ambient temperature air interacts accumulatively with the efficiency. Therefore, the efficiency tends to increase after a short period after decreasing solar incidence with higher temperatures. Therefore, the inlet temperature affects the efficiency at the end of the day. Figure 3 shows the temperature effect in experiments 7A and 7B, the efficiency increases at the end of the diurnal cycle.

Some factors indirectly affect the efficiency, and these parameters are related to the main factors to generate a general effect. For example, in the case of relative humidity, the amount diminishes during the day. The humidity combined with the low solar radiation and the air temperature increment provoke an increment effect of the efficiency almost at the end of the day; at the beginning of the solar cycle, the efficiency is high because of the low solar radiation. However, the accumulative effect of the other parameters increases the amount of efficiency.

The wind speed is one of the most unpredictable effects, with no apparent relation with the efficiency; the behavior is entirely random but was considered because it affects the hardware of the experiment, so it was added to the analysis. Since the inherent variability of the environmental parameters, some days have a non-intuitive behavior of efficiency. However, the effects in figure 2 to figure 4 show the Thermal efficiency performance concerning the environmental parameters.

3.2 Variance analysis results

Table 3 shows the average values of the daily thermal efficiency of the experiments carried out under the conditions described in Table 2. Significant differences in thermal efficiencies were observed between the run (A) and its repetition (B). The differences are associated with the effects of the prevailing environmental conditions during each experiment. Remarkably, there are differences in the thermal efficiency even with the same configuration. Figure

5 shows the variation of the incident solar radiation on the absorber plate in runs 2.A and 2.B, with their respective thermal efficiencies evaluated every 15 minutes. Thermal efficiencies show low values when solar radiation is maximum.

Previous studies found similar results regarding thermal efficiency: thermal efficiency is inverse to solar radiation (Heydari & Mesgarpour, 2018). This phenomenon is associated with the limited capacity of the absorber plate to transfer to the air or store a significant fraction of the incident energy. Under this condition, the excess of incident solar energy must be reflected outwards (Abuşka, 2018).

Table 3. Experimental design efficiencies.

Experiment number	Setting				h*100%	
	Plate depth	Plate material	Plate thickness	Air velocity		
1	1	1	1	1	1.A	26.68
					1.B	16.71
2	1	3	2	2	2.A	30.81
					2.B	52.75
3	1	2	3	3	3.A	48.38
					3.B	24.97
4	2	1	2	3	4.A	62.04
					4.B	28.01
5	2	3	3	1	5.A	15.13
					5.B	20.93
6	2	2	1	2	6.A	29.01
					6.B	34.28
7	3	1	3	2	7.A	13.96
					7.B	22.76
8	3	3	1	2	8.A	26.78
					8.B	15.98
9	3	2	2	1	9.A	65.58
					9.B	18.29

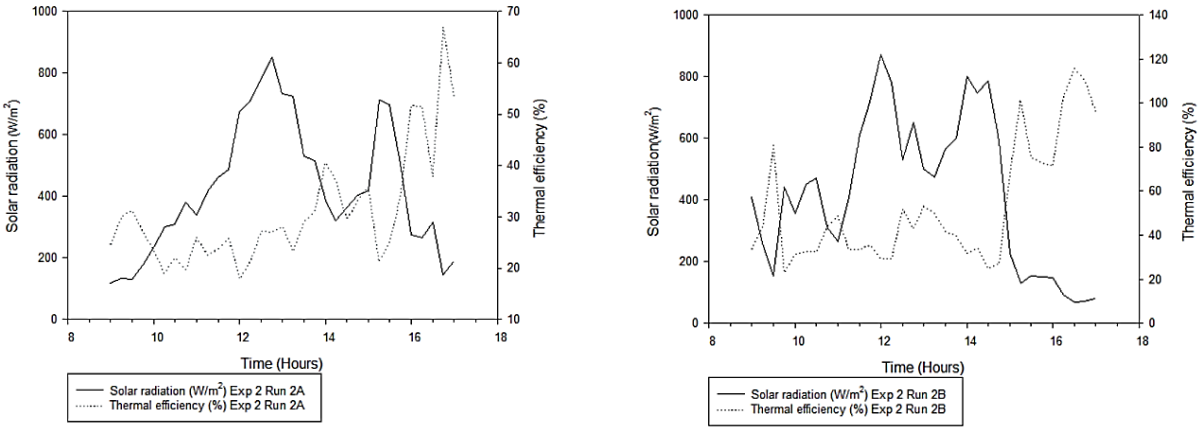

Figure 5. Variation of thermal efficiency and solar radiation under variable environmental conditions (Run 2A, October 16; Run 2B, November 12).

Table 4. Analysis of variance.

Variation sources	Degrees of freedom	Sum of squares	Mean of squares	F-value	P-Value
Plate depth	2	243.02	121.51	1.18	0.35
Plate material	2	25.63	12.81	0.12	0.884
Plate thickness	2	428.84	214.42	2.09	0.18
Air velocity	2	499.59	249.79	2.43	0.143
Error	9	924.02	102.67		
Total	17				

This effect is due to the low heat transfer rates between the absorber plate and the air, mainly due to the air's low thermal conductivity and little turbulence on the smooth surface of the absorber plate (Abuşka, 2018). The absorber plate's total mass and heat capacity are associated with the storage capacity of the incident solar energy. In the afternoon, the thermal efficiency increases slightly because the solar radiation decreases, and the absorber plate stores part of the previously absorbed energy. Also, some energy is meagerly transferred to the air. Heaters with energy storage systems consisting of plate-packed absorbers with meltable substances such as paraffin (Kabeel *et al*., 2017) can release absorbed energy from previous hours.

The effect of the design characteristics and configurations of absorber plates on thermal efficiency in heaters exposed to solar radiation and uncontrolled environmental conditions has been studied by several researchers (Heydari & Mesgarpour, 2018; Singh & Singh, 2018). However, the previous studies have not separated the effects of environmental conditions and the heaters' design characteristics or operating variables on thermal efficiency. Table 4 presents the analysis of variance of the design of experiments carried out, as the factor or source of variation with the highest sum of squares is the experimental error. The F statistic is the quotient between the variance associated with the effect of a factor and the variance due to experimental error (Means of squares). Even when plate thickness and velocity are the primary sources of variation considered, their sums of squares are not more significant than the experimental error. Because their confidence interval P indicates that they cannot be considered factors with a significant effect on thermal efficiency, this statistical relation indicates the need to use a more robust technique for data analysis.

The correlation analysis found that the environmental variables and factors considered in the design of experiments are not directly correlated with thermal efficiency. Solar radiation shows the most significant correlation coefficient -0.4458. Since there is a lack of data correlation, an ANN was proposed, improving data reproduction, and obtaining a simulation and data approximation tool.

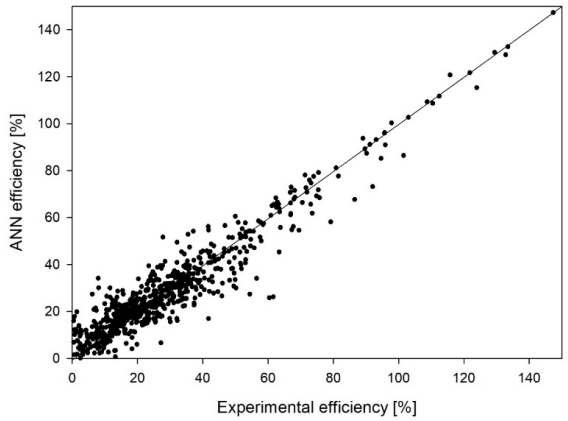

Figure 6. Correlation of the ANN model efficiency and the Experimental efficiency.

3.3 Artificial Neural Network Results

A Neural Network correlated thermal efficiency to environmental variables, design characteristics, and airspeed. When carrying out the network training described above, the simulated efficiency data were obtained, which presented a correlation of 96%. These data are presented in Figure 6. Figure 7 shows the experimental data and estimated thermal efficiency values using the developed neural network under the environmental conditions and those indicated in Table 2 of runs 2.A and 6.A. In experiment 2.A and 6.A the lowest and highest average solar radiations were recorded, 384 and 624 W/m^2, respectively. In the following sections, runs 6.A is identified as C1 and 2.A as C2.

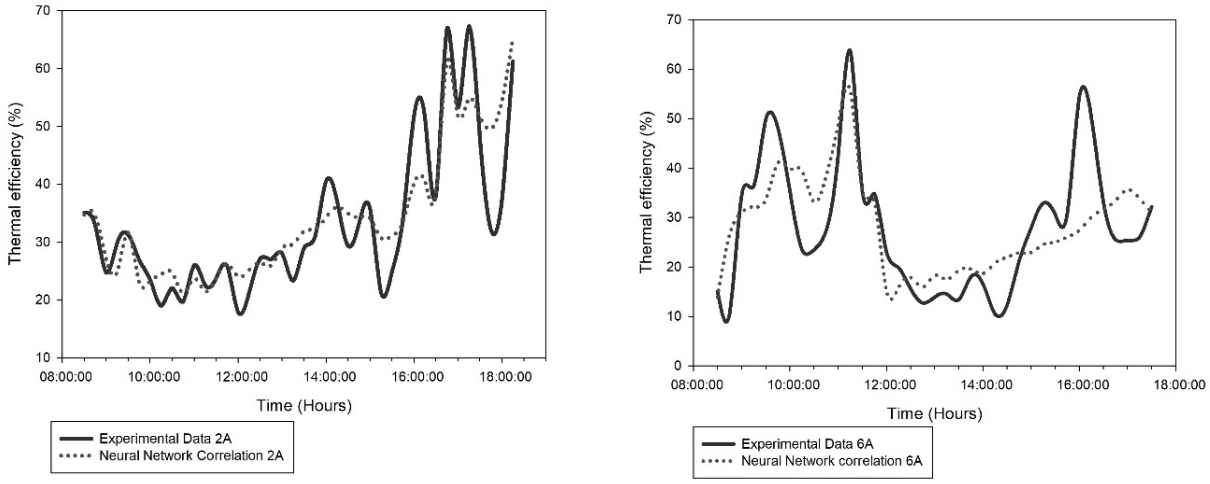

Figure 7. Runs 2.A and 6.A, with average radiations of 384 W/m^2 and 624 W/m^2.

Table 5. Average daily thermal efficiencies simulated by the neural network with low and high solar radiation.

Experiment number	Setting				Thermal efficiency	η *100%
	Plate depth	Plate material	Plate thickness	Air velocity		
1	1	1	1	1	Test 2A (Low irradiation)	38.49
					Test 6A (High irradiation)	10.11
2	1	3	2	2	Test 2A (Low irradiation)	30.47
					Test 6A (High irradiation)	24.06
3	1	2	3	3	Test 2A (Low irradiation)	72.29
					Test 6A (High irradiation)	83.34
4	2	1	2	3	Test 2A (Low irradiation)	117.84
					Test 6A (High irradiation)	89.98
5	2	3	3	1	Test 2A (Low irradiation)	39.09
					Test 6A (High irradiation)	63.42
6	2	2	1	2	Test 2A (Low irradiation)	56.74
					Test 6A (High irradiation)	31.51
7	3	1	3	2	Test 2A (Low irradiation)	55.58
					Test 6A (High irradiation)	31.16
8	3	3	1	3	Test 2A (Low irradiation)	94.95
					Test 6A (High irradiation)	69.33
9	3	2	2	1	Test 2A (Low irradiation)	44.81
					Test 6A (High irradiation)	27.92

The sets of the experimental design in Table 2 were simulated with ANN under constant environmental conditions. In addition, the environmental conditions of runs C1 and C2 were considered. Table 5 presents the results of the average daily thermal efficiencies obtained through simulation with the ANN. Most of the simulated runs at low solar radiation showed higher thermal efficiencies, in agreement with previous observations. However, in runs 3 and 5, the thermal efficiency was higher under high solar radiation. This last observation indicates that operating and design variables have an essential effect on thermal efficiency.

With the results of Table 5, the main effects of the operating variables were estimated: depth of the absorber plate and airflow velocity, and variables of material design and thickness of the absorber plate under the environmental conditions of runs C1 and C2. The calculation of the main effects shows again that the highest thermal efficiencies are generally reached at low solar radiation, Figures 8 and 9.

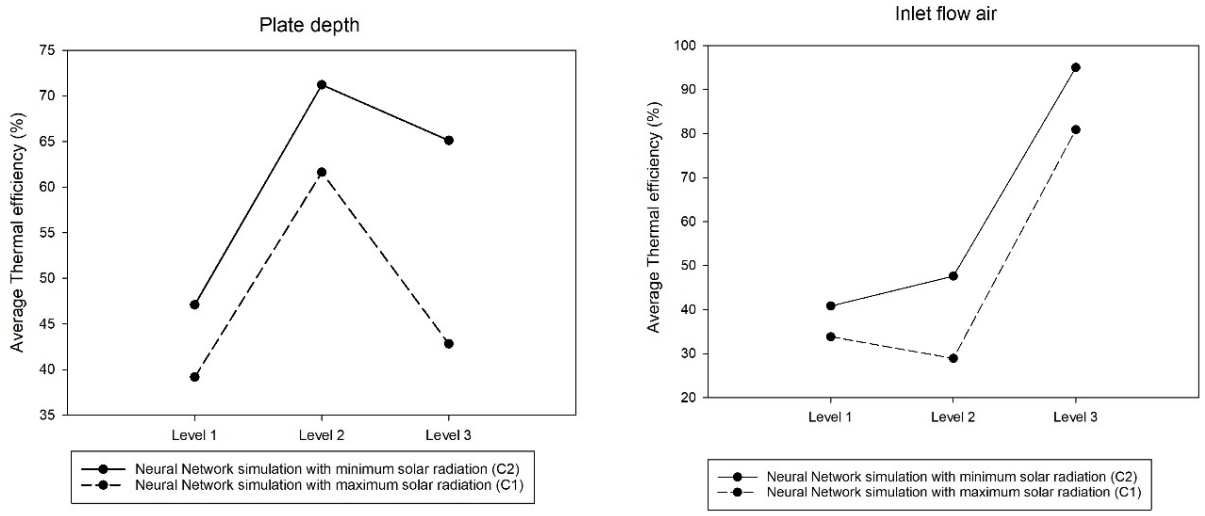

a) Plate depth b) Inlet flow air

Figure 8. Effect of the design parameters, plate depth (a) and inlet flow air (b), in the average thermal efficiency in days of maximum (C1) and minimum (C2) solar radiation.

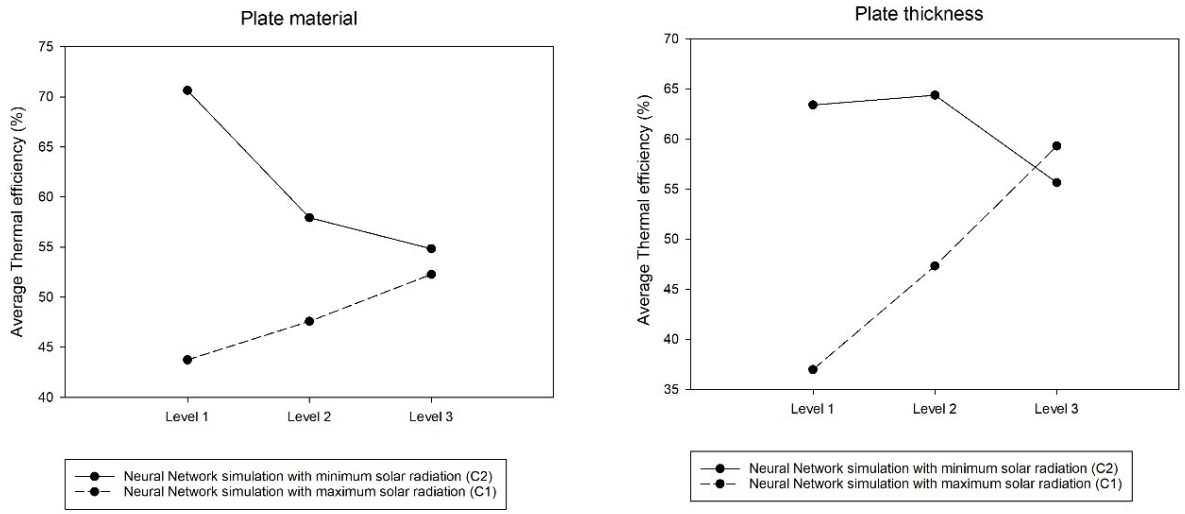

a) Plate material b) Plate thickness

Figure 9. Effect of the design parameters, plate material (a) and plate thickness (b), in the average thermal efficiency in days of maximum (C1) and minimum (C2) solar radiation.

However, it is also observed that there is an interaction effect of the operation and design variables with solar radiation. For example, Figure 8 shows that the primary outcomes of the placement of the absorber plate and the airflow in conditions of high and low solar radiation show similar behaviors: the placement of the absorber plate at a depth of 10cm and the greater airflow air increase thermal efficiency regardless of solar radiation.

Table 6. Effect of plate depth and air velocity on heat transfer coefficient.

Plate depth (m)	h (kW/m^2 K)	Inlet volumetric flow (m^3/s)	h (kW/m^2 K)
0.05	111.24	0.005067	77.16
0.1	98.38	0.007093	101.007
0.15	92.05	0.00912	123.48

Figure 9 shows the main effects of absorber plate material and thickness on thermal efficiency. These design variables show main results with opposite behaviors concerning high or low solar radiation. Aluminum plates (Level 3) deliver the best and worst performance in high and low solar radiation, respectively. In high solar radiation, greater thicknesses of the solar panel are preferred.

Air velocity and plate depth are two variables that substantially and complexly influence the heat transfer rate between the absorber plate and the air stream and the convective capacity of the air to remove heat from the heater air. The plate-air heat transfer rate is defined by the convective heat coefficient (h) related to the Nusselt number (Singh & Singh, 2018). The Nusselt number is associated with the air velocity through the Reynold number, already a characteristic length, which can be determined as the hydraulic radius of the solar heater's cross-section, defined by its width and the depth at which the absorber plate is placed. Table 6 evaluates the average effect of plate depth and volumetric inlet flow on the convective heat coefficient.

Table 6 shows the influence of plate depth and volumetric air flow on the heat transfer coefficient. With a most profound plate, the heat coefficient diminishes provoked by the lower contact of the surface air in the heated plate, and more air volume is needed to transfer heat. In the case of the volumetric inlet flow with a higher flow rate, the heat transfer coefficient increases, indicating the effect of turbulence in absorbing the plate's heat; this allows the plate to keep absorbing solar heat.

A fraction of solar energy is reflected in the surroundings by the absorber plate and the glass cover and losses by conduction or convection in other parts of the ASH. Another fraction is absorbed and accumulated to be later transferred to the air circulating on the plate surface. The amount of incident solar energy accumulated on the absorber plate depends on the amount of material and its thermophysical properties: density, specific heat capacity, and thermal conductivity.

In all the runs, the surfaces exposed to solar radiation of the absorber plates were painted with black acrylic enamel, so it was considered a constant factor in the analysis performed. However, the coating material may interact differently with the absorber plate material during heat transfer. Barrera-Calva *et al*. (2005) mention that the absorbance and emittance of the absorber plates change with the material and placement procedure of the coating.

El-Sebaii and Snani (2010) and Karwa and Srivastava (2013) proposed phenomenological mathematical models of heat transfer between the "cover film" of the absorber plate and the air. In their proposals, the heat transfer rates are governed by a balance of net absorbed energy, the energy transferred to the air, and the heat losses by different means. Under certain circumstances, heat transfer phenomena occur on the surface or at a shallow depth of the absorber plate. In these circumstances, neither the thickness nor the type of material of the absorber plate is relevant. When the solar incidence is intense, the excess energy is stored by the absorber plate to transfer to the air later. This phenomenon is applicable at the end of the experiments when the solar intensity decreases, Figure 7. In this period of time, the surface of the absorber plate is heated by solar incidence and the heat that emerges from the depth of the absorber plate.

3.4 Total average thermal efficiency simulated with Neural Network

This study aimed to create a methodology based on experiments and a mathematical model to identify the best configuration to improve the efficiency of a air solar heater whit flat plate absorber.

Figure 10 shows a simulated average efficiency considering the whole set of experiments. Figure 10 was made using the design parameters of each group, then simulated with the environmental conditions of all days. The results obtained give us the array option with the highest efficiency.

The best configuration acquired is Plate depth 0.15 [m], Plate material 76.2 [W/mK], Plate thickness 1.2 [mm], Airflow inlet 0.007 [m^3/s], with an average thermal efficiency of 61.3 %. This configuration is related to the effect of a combination of parameters; the plate depth has a medium level of efficiency,

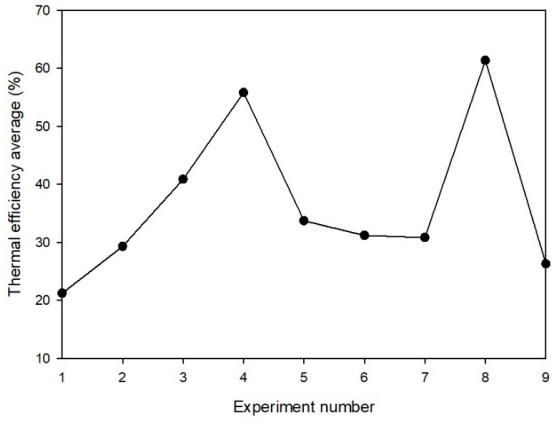

Figure 10. Average thermal efficiency simulated by Neural Network of all the environmental days in each design configuration.

the material corresponds to the medium absorber material with maximum solar radiation, the plate thickness corresponds to the highest efficiency in maximum solar radiation, and the inlet flow corresponds to the highest efficiency percent in the flow. This configuration indicates that a higher global thermal efficiency corresponds to average solar radiation. However, the second efficient configuration corresponds to the most efficient with lower radiation. It can be inferred that this Air Solar Heater of a flat plate is more efficient with lower solar radiation.

Conclusions

Analysis of variance was used to study the effect of design variables on the thermal efficiency of a WASH under the influence of uncontrolled environmental variables. The experimental error associated with the effect of the environmental conditionals exceeds the effects associated with the design characteristics, which means that these techniques in this case study do not yield a reliable result. The ANN allows for describing the system and identifying the significant parameters. The ANN is the tool used to analyze the efficiency of the absorber with respect to its design parameters even under variable environmental conditions.

The design parameters analyzed were the depth of the plates, the material from which the absorber plate is made, the thickness of the plate, and the volumetric airflow. When analyzing the results of the effect of these parameters on the thermal efficiency of solar air heaters, different conclusions were found at low and high solar radiation, mainly regarding the type of material and thickness of the absorber plates used. The increased solar radiation improves thermal efficiency with thicker aluminum plates, associated with a greater capacity for energy storage. The effects of the placement depth of the absorber plate and the airflow are similar in high and low radiation. These factors create hydrodynamic conditions that favor high surface-to-air heat transfer coefficients.

Efforts to improve the design and thermal efficiency of the absorber plate provided in ASH are to include air dispersal elements on the surface, improve the optical characteristics of the coating and increase its energy storage capacity. However, we find that the thermal efficiency of ASH strongly depends on the intensity of incident solar radiation, a non-controllable factor. Under this consideration, the new designs can include adaptive variables for a better use of the incident solar energy, such as the depth of the absorber plate and the air flow.

As a perspective of this work, it is considered to plan and solve a transport model, to study the interaction of the adsorbent surface coating and the metal plate during the heat transfer process. The active depth of the metal plate could be estimated at different intensities of solar radiation, with these results the observations made in this work could be explained.

Acknowledgement

This work was supported by the financing of the projects: “Tecnológico Nacional de México Proyect: 10150.21-P", “Tecnológico Nacional de México Project: 8988.20-P" and the acknowledgment to CONACYT for the scholarship granted 718087 and 710293

References

Abuşka, M. (2018). Energy and exergy analysis of solar air heater having new design absorber plate with conical surface. *Applied Thermal Engineering 131*, 115-124. https://doi.org/10.1016/j.applthermaleng.2017.11.129

Barrera-Calva, E., Martínez-Flores, J. C., Avila-García, A., Rodil, S., Huerta-Arcos, L., Viveros-García, T. (2005). Superficial characterization

of Co and Co-Fe oxide. *Revista Mexicana de Ingeniería Química 4*, 147-156. http://rmiq.org/ojs311/index.php/rmiq/article/view/2100

Bahrehmand, D., & Ameri, M. (2015). Energy and exergy analysis of different solar air collector systems with natural convection. *Renewable Energy 74*, 357-368. https://doi.org/10.1016/j.renene.2014.08.028

Compton, M., Willis, S., Rezaie, B., & Humes, K. (2018). Food processing industry energy and water consumption in the Pacific northwest. *Innovative Food Science and Emerging Technologies 47*(2017), 371-383. https://doi.org/10.1016/j.ifset.2018.04.001

Delfani, S., Esmaeili, M., & Karami, M. (2019). Application of artificial neural network for performance prediction of a nanofluid-based direct absorption solar collector. *Sustainable Energy Technologies and Assessments 36*(October), 100559. https://doi.org/10.1016/j.seta.2019.100559

Diez, F. J., Navas-Gracia, L. M., Martínez-Rodríguez, A., Correa-Guimaraes, A., & Chico-Santamarta, L. (2019). Modelling of a flat-plate solar collector using artificial neural networks for different working fluid (water) flow rates. *Solar Energy 188*(July), 1320-1331. https://doi.org/10.1016/j.solener.2019.07.022

El-Sebaii, A. A., Al-Snani, H. (2010). Effect of selective coating on thermal performance of plate solar air heaters. *Energy 35*, 1820-1828. https://doi.org/10.1016/j.energy.2009.12.037

Elsheikh, A. H., Sharshir, S. W., Abd Elaziz, M., Kabeel, A. E., Guilan, W., & Haiou, Z. (2019). Modeling of solar energy systems using artificial neural network: A comprehensive review. *Solar Energy 180*(January), 622-639. https://doi.org/10.1016/j.solener.2019.01.037

Heydari, A., & Mesgarpour, M. (2018). Experimental analysis and numerical modeling of solar air heater with helical flow path. *Solar Energy 162*(November 2017), 278-288. https://doi.org/10.1016/j.solener.2018.01.030

IRENA. (2020). *Renewable Energy Can Support Resilient and Equitable Recovery*. https://www.irena.org/newsroom/pressreleases/2020/Apr/Renewable-energy-can-support-resilient-and-equitable-recovery

Karwa, R., Srivastava, V. (2013). Thermal performance of solar air heater having absorber plate with V - Down discrete rib roughness for space - heating applications. *Journal of Renewable Energy*.1-13. http://dx.doi.org/10.1155/2013/151578

Kabeel, A. E., Hamed, M. H., Omara, Z. M., & Kandeal, A. W. (2017). Solar air heaters: Design configurations, improvement methods and applications - A detailed review. *Renewable and Sustainable Energy Reviews 70*(December), 1189-1206. https://doi.org/10.1016/j.rser.2016.12.021

Kumar, M., Sansaniwal, S. K., & Khatak, P. (2016). Progress in solar dryers for drying various commodities. *Renewable and Sustainable Energy Reviews 55*, 346-360. https://doi.org/10.1016/j.rser.2015.10.158

Liao, W., Heo, Y., & Xu, S. (2019). Simplified vector-based model tailored for urban-scale prediction of solar irradiance. *Solar Energy 183*(August 2018), 566-586. https://doi.org/10.1016/j.solener.2019.03.023

ONU. (2015). Energía asequible y no contaminante. https://www.un.org/sustainabledevelopment/es/energy/

Montgomery, D. C. (2004). *Diseño y Análisis de Experimentos*. Segunda Edición. Editorial Limusa S.A. de C.V. México.

Sanjuan, N., Stoessel, F., & Hellweg, S. (2014). Closing data gaps for LCA of food products: Estimating the energy demand of food processing. *Environmental Science and Technology 48*(2), 1132-1140. https://doi.org/https://doi.org/10.1021/es4033716

Sharma, A., Shukla, A., & Aye, L. (Eds.). (2018). Low Carbon Energy Supply. Springer Singapore. https://doi.org/10.1007/978-981-10-7326-7

Singh Bisht, V., Kumar Patil, A., & Gupta, A. (2018). Review and performance evaluation of roughened solar air heaters. *Renewable and Sustainable Energy Reviews 81*(August 2017), 954-977. https://doi.org/10.1016/j.rser.2017.08.036

Singh, I., & Singh, S. (2018). A review of artificial roughness geometries employed in solar air heaters. *Renewable and Sustainable Energy Reviews 92*(December 2017), 405-425. https://doi.org/10.1016/j.rser.2018.04.108

Sowmy, D. S., Schiavon Ara, P. J., & Prado, R. T. A. (2017). Uncertainties associated with solar collector efficiency test using an artificial solar simulator. *Renewable Energy 108*, 644-651. https://doi.org/10.1016/j.renene.2016.08.054

Sözen, A., Menlik, T., & Ünvar, S. (2008). Determination of efficiency of flat-plate solar collectors using neural network approach. *Expert Systems with Applications 35*(4), 1533-1539. https://doi.org/10.1016/j.eswa.2007.08.080